Pakistan Veterinary Journal

ISSN: 0253-8318 (PRINT), 2074-7764 (ONLINE)
DOI: 10.29261/pakvetj/2025.312

RESEARCH ARTICLE

Characterization and Vaccine Potential of *Et*RON2$_{L1-1}$, a Novel RON2 Paralog in *Eimeria tenella*

Wenqiang Tang[1*], Manyu Liu[2], Xialing Zhao[2], Bin Shi[1], Wanxiang Qi[1], Hui Dong[2] and Kun Li[3]

[1]Institute of Animal Science, Xizang Academy of Agricultural and Animal Husbandry Sciences, Lhasa 850009, PR China; [2]Shanghai Veterinary Research Institute, Chinese Academy of Agricultural Sciences, Key Laboratory of Animal Parasitology of Ministry of Agriculture, Minhang, Shanghai 200241, PR China; [3]College of Veterinary Medicine, Nanjing Agricultural University, Nanjing 210095, PR China.
*Corresponding author: tang.iwate@gmail.com

ARTICLE HISTORY (25-788)

Received: August 06, 2025
Revised: November 07, 2025
Accepted: November 10, 2025
Published online: December 09, 2025

Key words:
Eimeria tenella
Host cell invasion
Rhoptry neck protein
Vaccine candidate

ABSTRACT

Eimeria (*E.*) *tenella*, the causative agent of avian coccidiosis, employs apical complex proteins like RON2 for host cell invasion. While *Et*RON2 has been well-studied, its paralogs remain poorly characterized. This study investigated *Et*RON2$_{L1-1}$, a RON2 homolog, for its structural features, stage-specific expression, and vaccine potential. Bioinformatic analysis revealed *Et*RON2$_{L1-1}$ shares only 23.46% amino acid identity with *Et*RON2, lacks a signal peptide, and contains three transmembrane domains. Expression profiling revealed distinct transcriptional and translational regulations, with peak mRNA levels in sporulated oocysts and highest protein expression in sporozoites, indicative of post-transcriptional control. Immunofluorescence studies showed stage-dependent localization patterns: cytoplasmic distribution in free sporozoites transitioning to apical end during host cell invasion. In vitro neutralization assays established *Et*RON2$_{L1-1}$'s involvement in invasion, with specific antibodies exhibiting dose-dependent inhibition (13% at 50µg/mL to 42% at 400µg/mL). Vaccination trials demonstrated that while 100µg pCAGGS-*Et*RON2$_{L1-1}$ significantly improved weight gain and reduced oocyst output compared to controls, its protective efficacy was inferior to pCAGGS-*Et*RON2$_{L2}$, particularly in mitigating intestinal lesions. These findings characterize *Et*RON2$_{L1-1}$ as a functionally distinct RON2 paralog involved in host cell invasion, with partial but promising vaccine potential that requires further optimization for effective coccidiosis control.

To Cite This Article: Tang W, Liu M, Zhao X, Shi B, Qi W, Dong H and Li K, 2025. Characterization and vaccine potential of *Et*RON2$_{L1-1}$, a novel RON2 paralog in *Eimeria tenella*. Pak Vet J. http://dx.doi.org/10.29261/pakvetj/2025.312

INTRODUCTION

Apicomplexan parasites, including *Toxoplasma* (*T.*) *gondii*, *Plasmodium* spp., *Babesia* spp., *Eimeria* (*E.*) spp., and *Cryptosporidium* spp., are significant pathogens affecting both humans and animals, posing serious threats to public health and livestock production (Robert-Gangneux and Dardé, 2012). These protozoans possess specialized secretory vesicles known as apical organelles, which include rhoptries, micronemes, and dense granules. These structures facilitate a highly conserved mechanism for host cell invasion (Blackman and Bannister, 2001; Dubois and Soldati-Favre, 2019). During invasion, Rhoptry Neck Protein 2 (RON2), secreted by rhoptries, adheres to and embeds itself into the host cell membrane. It then interacts with Apical Membrane Antigen 1 (AMA1), a microneme-derived protein, to form the AMA1-RON2 complex (Parker and Boulanger, 2015). This complex localizes to the moving junction (MJ) and plays a critical role in host cell entry. The disruption of AMA1-RON2 interaction ceases the parasite invasion, making these proteins vaccine candidates (Ishino *et al*., 2019; Lee *et al*., 2023). Recent studies have revealed that, in addition to the well-characterized AMA1 and RON2, Eimeriorina parasites (*Toxoplasma*, *Eimeria*, and *Neospora*) possess three AMA1 homologs (AMA2, AMA3, and AMA4) and at least two RON2 homologs (RON2$_{L1}$ and RON2$_{L2}$). These proteins form corresponding complexes: AMA2-RON2, AMA3-RON2$_{L2}$, and AMA4-RON2$_{L1}$ (Parker *et al*., 2016). However, the precise functions of these alternative complexes remain poorly understood.

Eimeria tenella, the primary causative agent of chicken coccidiosis, undergoes extracellular sporogony

followed by intracellular schizogony and gametogony during its life cycle (Lillehoj and Trout, 1993). Proteomic analyses of *E. tenella* sporozoite rhoptries and stage-specific proteins have identified four *Et*RON2 family members (*Et*RON2, *Et*RON2$_{L1-1}$, *Et*RON2$_{L1-2}$, and *Et*RON2$_{L2}$), each exhibiting stage-specific expression patterns: *Et*RON2 is expressed in sporozoites and second-generation schizonts, *Et*RON2$_{L1-1}$ and *Et*RON2$_{L2}$ are primarily active in sporozoites, while *Et*RON2$_{L1-2}$ is likely associated with schizont stages (Lal *et al*., 2009; Oakes *et al*., 2013). Phylogenetic analyses suggest specific interactions between *Et*RON2 variants and apical membrane antigens (*Et*AMAs): *Et*RON2 with *Et*AMA1/3, *Et*RON2$_{L2}$ with *Et*AMA3, *Et*RON2$_{L1-1}$ /*Et*RON2$_{L1-2}$ with *Et*AMA4 (Parker *et al*., 2016). The interaction between *Et*RON2 and *Et*AMA1 was confirmed by both yeast two-hybrid (Han *et al*., 2016) and BiFC assays (Yan *et al*., 2019). Further studies localized *Et*RON2 to the apical end of *E. tenella* sporozoites and merozoites, and antibodies targeting *Et*RON2 were shown to inhibit parasite invasion of host cells and intestinal epithelium (Wang *et al*., 2020; Li *et al*., 2024). The vaccine potential of *Et*RON2 protein is evidenced by the superior protection conferred by *Et*RON2-expressing *Lactobacillus plantarum* compared to commercial vaccines (Zhang e*t al*., 2024).

While *Et*RON2 has been extensively studied, its paralogs remain poorly characterized. Among these, *Et*RON2$_{L2}$ displays particularly distinct features, sharing only 26.63% sequence identity with *Et*RON2. This paralog undergoes dynamic relocalization from cytoplasmic to surface exposure during sporozoite invasion, and functional studies demonstrate both its critical role in host cell penetration (as evidenced by invasion inhibition with specific antibodies) and its physical interaction with *Et*AMA3 (Liu e*t al*., 2024). To expand our understanding of this protein family, we systematically investigated *Et*RON2$_{L1-1}$, examining its structural characteristics, biological functions, and immunological properties. These studies not only assess its vaccine potential but also provide new insights into the functional diversification of RON2 family members in *Eimeria* species.

MATERIALS AND METHODS

***Et*hics statement:** The present study was approved by the Animal *Et*hics Committee of the Shanghai Veterinary Institute, Chinese Academy of Agricultural Science. All Experiments were performed following *Et*hical guidelines and approved protocols for animals (Permit Number: SHVRI-SZ-20230622-5).

Experimental design: The experimental chickens were raised in a coccidia-free environment, and no anti-coccidial drugs were added to the diet and drinking water. 8-week-old New Zealand white rabbits were purchased from Shanghai Jiagan Biotechnology Co., LTD. The Shanghai strain of *E. tenella* (resource number: CAAS21111611), the chicken fibroblast cell line DF-1, and BKH cells were procured from the Shanghai Veterinary Research Institute, CAAS. The unsporulated oocysts (UO), sporulated oocysts (SO), sporozoites, and second-generation merozoites (Mrz) of *E. tenella* were collected and purified following established protocols (Zhou *et al*., 2010; Walker *et al*., 2015; Wang *et al*., 2021).

Sequence analysis of *Et*RON2$_{L1-1}$: The VEuPathDB (https://veupathdb.org/veupathdb/app/) website was used to download the *Et*RON2$_{L1-1}$ (Gene ID: *ET*H_00013625) gene and protein sequences. Basic physicochemical information, such as amino acid (AA) composition, isoelectric point, and molecular weight, was obtained by using ExPASy-PortParam. The transmembrane (TM) and signal peptide domains were identified through predictions made by SignalP (v6.2) and TMHMM (v2.0), respectively. Multiple sequence alignment was performed using the ClustalW program. *Et*RON2$_{L1-1}$ homologous protein sequences were identified using the Blastp. Signal peptide and transmembrane domains were predicted using SignalP v6.0, Phobius, and SecretomeP 2.0. Multiple sequence alignment (MSA) was conducted using Clustal Omega, and a phylogenetic tree was generated using MEGA-X with the Neighbor-Joining method and 1000 bootstrap replicates to assess evolutionary relationships among RON2 family members.

Amplification, cloning, and sequencing of the truncated *Et*RON2$_{L1-1}$ gene: To avoid the hydrophobic transmembrane domains (predicted at residues 351-373, 390-412, and 483-505), a C-terminal truncated fragment of *Et*RON2~$_{L1-1}$ ~ corresponding to 1-246AA was amplified for recombinant expression. Designing of primers was aimed to amplify the C-terminally truncated *Et*RON2$_{L1-1}$ fragments, based upon the *Et*RON2$_{L1-1}$ gene sequences that were deposited in the relevant database (GenBank No.: XM_013378450.1). The primers used were: forward primer: 5'-CGGGATCCATGGCATTTACT CGCTCAGA-3', and reverse primer: 5'-CGGAATTCGGA GTCGGTCTTCCTTCGG-3', and *BamHI* and *EcoRI* restriction sites were added to the upstream and downstream primers (underlined). Extraction of total RNA of sporulated oocysts was performed using the MiniBEST Universal RNA Extraction Kit (TaKaRa, Tokyo, Japan). Synthesis of cDNA was performed from the total RNA using the M-MLV reverse transcriptase kit. *Et*RON2$_{L1-1}$ was amplified by RT-PCR. 1% agarose gel was used to detect the PCR product, cloned into the pGEM-T-Easy vector, and transformed into TOP10. Positive clones were picked and identified by PCR. The sequence integrity of the correctly identified recombinant plasmid clones was confirmed by DNA sequencing.

Expression and purification of recombinant truncated *Et*RON2$_{L1-1}$ protein: The correct sequenced plasmid was digested with *BamHI* and *EcoRI*, and cloning was done into the pGEX-4T-1 vector (purchased from Novagen, Darmstadt, Germany), digested (double) with restriction enzymes. The plasmid (recombinant) was identified and confirmed as positive by PCR, double enzyme digestion, and sequencing, and then the recombinant plasmid was introduced into B$_{L2}$1 (DE3) (Tiangen, Beijing, China). 1.0mmol/L IPTG (isopropyl-β-D-thiogalactopyranoside) was used to induce the expression of recombinant protein; the bacterial solution was sonicated and then subjected to SDS-PAGE electrophoresis, stained, and decolorized to determine whether the recombinant protein (r*Et*RON2$_{L1-1}$)

was expressed and in its expression form. The induced recombinant protein was mainly expressed in inclusion bodies and was purified by cutting the gel. The required amount was estimated by the BCA protein concentration determination kit, and placed at -20°C for later use.

Immunogenicity analysis: The purified recombinant protein was analyzed by SDS-PAGE, then shifted to PVDF membrane, and skimmed milk (5%) was used to block, followed by 3 times washing with PBS. Anti-sporozoite serum (diluted 1:100, prepared by our laboratory) and rabbit negative serum (diluted 1:100) were utilized as primary antibodies, incubated at 25°C for 1h, followed by washing 5 times with TBST, 5 min each time. The HRP-labeled goat anti-rabbit IgG (diluted 1:5000) was used as a secondary antibody, incubated at room temperature for 45min. Five times after washing with TBST, the membrane was incubated with developer solution for 2min, then imaged with ChemiDoc TMTouch protocol for imaging.

Preparation of polyclonal antibody of r*Et*RON2$_{L1\text{-}1}$: Purified r*Et*RON2$_{L1\text{-}1}$ (0.2mg) was mixed with an equal volume of Freund's complete adjuvant, and subcutaneous immunization was given to 2.5kg New Zealand white rabbits, and 0.05mg recombinant protein was administered to 6-wk-old mice. The rabbits or mice were provided with a booster dose three times every 2 weeks with the same amount of recombinant protein emulsified in Freund's incomplete adjuvant. A week after the last immunization, blood samples were obtained, serum was separated, and stored at -20°C.

RT-PCR assay: The extraction of total RNAs of UO, SO, SPZ, and MRZ was performed, and then contaminating DNA was removed using DNase I (TaKaRa). Then, SuperScript™ II Reverse Transcriptase was used to synthesize the first strand of cDNA and random primers, and was used as a template for real-time RT-PCR. The *Et*RON2$_{L1\text{-}1}$ primer sequences were as follows: forward primer: 5'-GAGTCGGTCTTCCTTCGGCAATG-3', reverse primer: 5'-TGTCATCTGGAGGACCACTTGGG-3'. The 18S rRNA housekeeping gene of *E. tenella* (forward: 5'-TGTAGTGGAGTCTTGGTGATTC-3'; and reverse primer: 5'-CCTGCTGCCTTCCTTAGATG-3') was utilized to play the role of a unified reference gene (Jiang *et al*., 2012). The RT-PCR was performed in the 7500 Fast Real-Time PCR System according to the instructions of One Step TB Green PrimeScriptTM RT-PCR Kit II (Perfect Real Time) (TaKaRa). The reaction system was as follows: One Step TB Green RT-PCR Buffer 4 (2X) 10μL, TaKaRa Ex TaqHS (5U/μL) 0.4μL, PrimeScript 1 Step Enzyme Mix II 0.4μL, Forward Primer (10μM) 1μL, Reverse Primer (10μM) 1μL, ROX Reference Dye or Dye II (50X) 0.4μL, Total RNA 2μL, RNase Free ddH2O 4.8μL. The parameters that were used in qPCR are given in Table 1. Every experiment was performed three times using three replicates for each. Relative variations in gene expression were enumerated using the $2^{-\Delta\Delta Ct}$ protocol (Geysen *et al*., 1991).

Western blot analysis: The proteins of SPZ, SO, UO, and MRZ were extracted with RIPA (strong) lysate, and the amount of protein was estimated using the BCA kit protocol. The SDS-PAGE was used to fractionate a sample of the four-stage protein. Proteins separated by Gel were shifted to a PVDF membrane, blocking was done with skim milk as mentioned earlier, and incubation was done in r*Et*RON2$_{L1\text{-}1}$-antibodies containing rabbit sera (1:100 dilution). Murine monoclonal anti-α-tubulin diluted to 1:3000 was also used as a reference for each group. Next, HRP-labeled caprine anti-rabbit IgG or goat anti-mouse IgG (1:3000 dilution) was added, and the protein-antibody complexes were visualized.

Table 1: qRT-PCR Cycling Conditions

Step	Process	Temperature	Time	Cycles
1	Reverse Transcription	42°C	5min	1
2	Initial Denaturation	95°C	10sec	1
3	Amplification	95°C	5sec	40
		60°C	34sec	
4	Melting Curve Analysis	95°C	15sec	1
		60°C	34sec	
		95°C	15sec	

Indirect Immunofluorescent Assay (IFA): IFA was used to study the distribution of *Et*RON2$_{L1\text{-}1}$ protein in sporozoites (SZ), immature and mature schizonts, and second-generation merozoites (SM) of *E. tenella*. After purification, SM and SZ were shifted to slides made up of glass dried in air. 1.0×10^6 DF-1 cells per well were initially went through incubation in 6-well plates with already coated glass coverslips and cultured in 5% CO_2 incubator at 37ºC until the cells' coverage became 80%~90%. The addition of sporozoites was then carried out to the cells according to the ratio of sporozoites to cells 2:1 (MOI=2) and cultured in an incubator at 37ºC and 5% CO_2. At 2, 60, and 72h, the six-well plate was taken out, and the fixation of cells was carried out with 4% paraformaldehyde for half an hour, using 1% Triton X-100 for permeabilization for a period of 20min, and then blocking was carried out with 2% (w/v) bovine serum albumin in PBS for 2h at 37ºC. Rabbit anti-r*Et*RON2$_{L1\text{-}1}$ polyclonal antibody (1:100) was added and incubated at 37°C for 2h. After washing 3 times with PBST, Alexa Fluor® 488 Goat Anti-Rabbit IgG (diluted 1:500) was added and incubated at 25ºC for 1h. After washing 3 times with PBST, DAPI was added for staining the nuclei at 25ºC for a quarter of an hour, and the addition of anti-fluorescence quencher (dropwise) was performed thereafter, and the cells were examined through fluorescence microscopy (Olympus, Tokyo, Japan).

Invasion inhibition assays: Briefly, DF-1 cells (1.0×10^5 cells/well) were added to a 24-well plate and cultured in a 37ºC, 5% CO_2 incubator until the cell coverage became about 80%~90%. The purification of anti-r*Et*RON2$_{L1\text{-}1}$ polyclonal antibody was carried out through Protein A+G Agarose, and the amount was estimated by the BCA method. After labeling with CFDA SE (1:20000) (Beyotime) for 15min, the incubation of fresh sporozoites was performed at 37°C for 2h with 50, 100, 200, 300, and 400μg/ml purified antibody. Then, the sporozoites were added to the cells at a ratio of 3:1 (MOI=3) and cultured in an incubator at 37°C with 5% CO_2 for one-third of a day. The Cytomics FC500 flow cytometer detected the invasion of sporozoites. Normal rabbit IgG of the same concentration was used as a negative

control, and cells without antibody incubation were used as a positive control.

Construction and expression of pCAGGS-*Et*RON2$_{L1-1}$ /pCAGGS-*Et*RON2$_{L2}$ plasmids: The partial fragment of *Et*RON2$_{L1-1}$ and *Et*RON2$_{L2}$ (Gene ID: *ET*H_00028240, as a reference control) (1935 bp) genes amplification was carried out with the following primers: *Et*RON2$_{L1-1}$ SP: 5'-CATCATTTTGGCAAAGAATTCGGATGGCATTTAC TCGCTCAGAAAA-3', *Et*RON2$_{L1-1}$ AP: 5'-TGCGGCC GCGAGCTCGAATTCGAGTCGGTCTTCCTTCGGCA-3'; *Et*RON2$_{L2}$ SP: 5'-CATCATTTTGGCAAAGAATTC CCGACTGCTATTCTCTCGCTG-3', *Et*RON2$_{L2}$ AP: 5'-TGCGGCCGCGAGCTCGAATTCTTGACCACCATCA GCTTTCAATT-3'; *EcoRI* restriction site was added to the upstream and downstream primers (underlined). The products obtained after performing PCR were cloned into the pCAGGS vector and were aligned as pCAGGS-*Et*RON2$_{L1-1}$ and pCAGGS-*Et*RON2$_{L2}$. The constructed plasmid was detected to possess the right configuration through performing sequencing and was purified using a Qiagen Plasmid Giga Kit. To determine the concentration of the plasmid, spectrophotometry was performed.

A single layer of DF-1 cells at 80-90% confluence was transduced through transfection with 4μg of pCAGGS-*Et*RON2$_{L1-1}$, pCAGGS-*Et*RON2$_{L2}$, or the empty pCAGGS vector using Lipofectamine 2000 (Invitrogen). The DNA and transfection reagent were prepared by mixing 4μg of DNA with 10μl of Lipofectamine 2000, then incubated at 25°C for half an hour to apply to the cells. After six hours, the mixture was changed with DMEM supplemented with 10% FBS. After 48h of transfection, the expression of *Et*RON2$_{L1-1}$ or *Et*RON2$_{L2}$ proteins was verified by indirect immunofluorescence assay (IFA) using specific antibodies against *Et*RON2$_{L1-1}$ or *Et*RON2$_{L2}$, following the protocol described by Li *et al*. (2013).

DNA vaccination and challenge infection in chickens: 7-day-old chicks (n=112) were classified into eight groups, each having 14 chicks. The first three groups were vaccinated with 50μg of pCAGGS-*Et*RON2$_{L1-1}$, pCAGGS-*Et*RON2$_{L2}$, and pCAGGS, mixed in TE buffer. Groups 4, 5, and 6 were immunized with 100μg of pCAGGS-*Et*RON2$_{L1-1}$, pCAGGS-*Et*RON2$_{L2}$, and pCAGGS added in TE buffer. Groups 7 and 8 were injected with sterile TE buffer at the identical location of injection and were nominated as a positive control, while the non-challenged group served as a negative control. All the experimental birds were vaccinated by IM injections in the leg, and a booster dose was given by the same route and dosage after one week. At 21 days post-immunization, all chickens except the unchallenged control group were inoculated orally with 1×10^4 sporulated oocysts of *E. tenella* (Shanghai strain).

Seven days after the challenge infection, all the chickens were weighed individually and slaughtered for lesion score according to the method of Johnson and Reid (1970). Additionally, oocyst shedding per bird on days 6 to 8 after challenge was determined using a McMaster chamber (Sun *et al*., 2014). The Protective efficacy was analyzed based on the survival rate, body weight, lesion scoring, and oocyst reduction ratio as described previously (Dong *et al*., 2016; Song *et al*., 2017).

Statistical analysis: All experimental data were analyzed using SPSS Statistics for Windows, Version 22.0. Group differences were assessed through Duncan's multiple range tests. A significance level of $0.01 < P<0.05$ was denoted by a single asterisk (*), $0.001 <P<0.01$ was indicated by two asterisks (**), and $P<0.001$ was marked with three asterisks (***), demonstrating increasing levels of statistical significance. In the figures, different letters denote statistically significant differences between groups at $P<0.05$.

RESULTS

Analysis of the *Et*RON2$_{L1-1}$ gene: The mRNA sequence of *E. tenella Et*RON2$_{L1}$ (Gene ID: *ET*H_00013625) was predicted to be 1710bp in length, encoding a 569AA protein with a molecular weight of 63.398kDa and a theoretical isoelectric point of 9.52. Bioinformatic analysis revealed that the *Et*RON2$_{L1-1}$ protein lacks a signal peptide but contains three transmembrane regions: 351-373, 390-412, and 483-485AA. Additional signal peptide prediction using SignalP v6.0 and Phobius confirmed the absence of a canonical N-terminal signal sequence in *Et*RON2$_{L1-1.}$ However, SecretomeP analysis indicated a non-classical Secretion potential (NN-score 0.68), suggesting that *Et*RON2$_{L1-1}$ may be secr*et*ed via a non-classical pathway. Similar non-classical secr*et*ion mechanisms have been reported for certain rhoptry-associated proteins in Apicomplexa lacking conventional signal peptides. Sequence alignment demonstrated that the *Et*RON2$_{L1-1}$ AA sequence shares 23.46% identity (71% query coverage) with *E. tenella* canonical RON2 (Gene ID: *ET*H_00012760), 30.74% identity (46% query coverage) with *E. tenella Et*RON2$_{L1}$ paralog (Gene ID: *ET*H_00030325), 36.36% identify (query coverage, 88%) with *T. gondii* RON2$_{L1}$ (Gene ID: TGME49_294400) and 34% identify (query coverage, 97%) with *Neospora caninum* RON2$_{L1}$ (Gene ID: NCLIV_001400). To confirm the evolutionary relationship, a multiple sequence alignment (MSA) was performed using Clustal Omega with canonical *Et*RON2, *Et*RON2$_{L1-1,}$ *Et*RON2$_{L2}$, and RON2 homologs from *T. gondii* and *Neospora caninum*. Conserved motifs, including transmembrane and partial AMA1-interacting regions, were identified among all sequences. Phylogen*et*ic analysis based on full-length AA sequences (Neighbor-Joining, 1000 bootstrap replications) showed that *Et*RON2$_{L1-1}$ and *Et*RON2$_{L2}$ cluster tog*et*her within a distinct RON2 family branch, confirming their classification as RON2 paralogs.

Expression and purification of truncated r*Et*RON2$_{L1-1}$ protein: The *Et*RON2$_{L1-1}$ protein contains three transmembrane domains located at the following sites: 351-373, 390-412, and 483-485AA. To avoid these hydrophobic regions, we expressed a C-terminal truncated version of *Et*RON2$_{L1-1}$ (246AA, corresponding to 738bp), with a predicted molecular weight of 27.0kDa.

Using *E. tenella* sporulated oocyst cDNA as template, we successfully amplified a 738bp fragment by PCR (Fig.1A). The truncated *Et*RON2$_{L1-1}$ was expressed in *E. coli* as a GST-tagged fusion protein following induction with 1mmol/L IPTG for 2-8hrs. SDS-PAGE analysis revealed a recombinant protein band between 43-

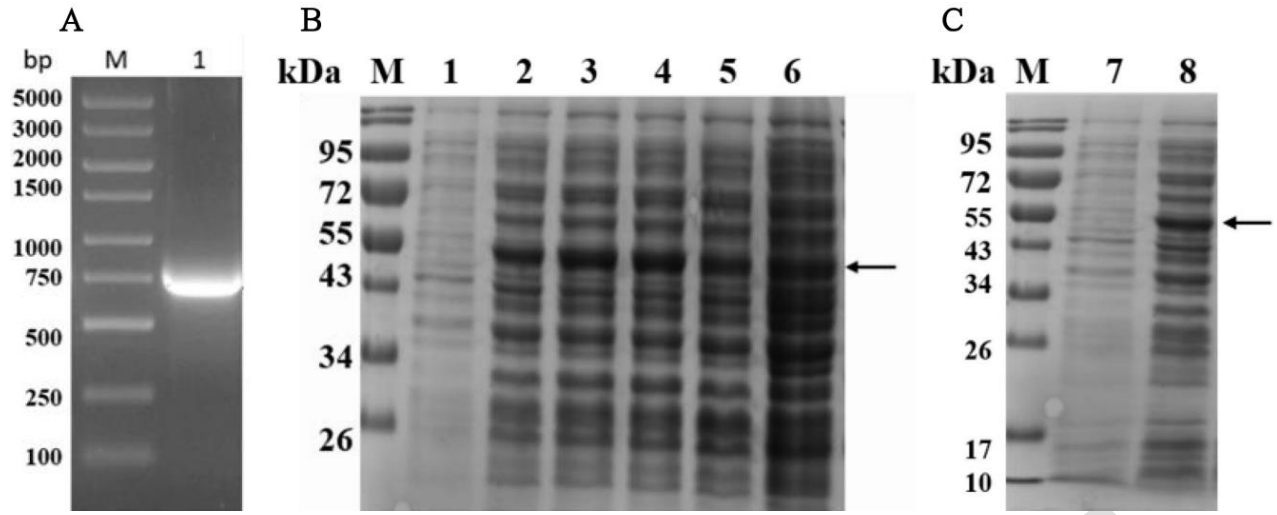

Fig. 1: Cloning and expression of truncated *Et*RON2$_{L1-1}$. A. The PCR result of *Et*RON2$_{L1-1}$. M: DNA marker; 1: *Et*RON2$_{L1-1}$. B. SDS-PAGE confirms the expression of recombinant truncated *Et*RON2$_{L1-1}$ protein. M: Marker, 1-6: Protein expressed in 0, 2, 4, 6, 8, 10h. C: Expression forms of r*Et*RON2$_{L1-1}$. M: Marker, 7: Supernatant of r*Et*RON2$_{L1-1}$, 8: Inclusion body of r*Et*RON2$_{L1-1}$.

55kDa (Fig. 1B), consistent with the expected size (53kDa; comprising 27kDa *Et*RON2$_{L1-1}$ and 26kDa GST tag) and was mainly expressed in the inclusion body (Fig. 1C). The recombinant protein was specifically recognized by rabbit anti-sporozoite serum, while no reactivity was observed with naïve rabbit sera (Fig. 2).

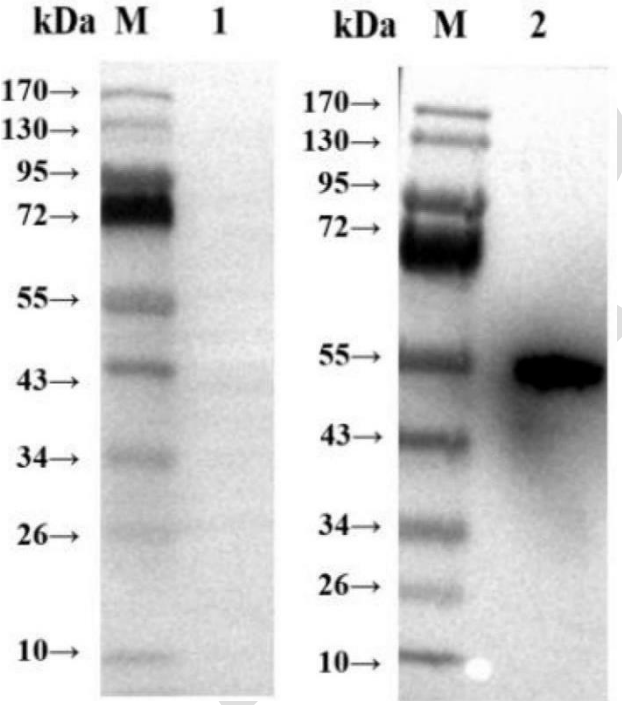

Fig. 2: Western blot analysis of purified r*Et*RON2$_{L1-1}$. Rabbit antiserum targeting *Eimeria tenella* sporozoites served as the primary antibody. In lane 1, r*Et*RON2$_{L1-1}$ was tested with serum from a naive rabbit, while lane 2 showed r*Et*RON2$_{L1-1}$ probed with serum from a rabbit immunized against sporozoites.

Stage-specific expression profile of *Et*RON2$_{L1-1}$ in *E. tenella*: Developmental analysis of *Et*RON2$_{L1-1}$ revealed distinct transcriptional and translational regulation across life cycle stages. qPCR demonstrated peak mRNA expression in sporulated oocysts ($P<0.05$ versus other stages), while unsporulated oocysts, sporozoites, and merozoites showed comparable transcription levels ($P>0.05$) (Fig. 3A). Western blot analysis of the ~72kDa protein detected discordant translation patterns, with sporozoites exhibiting maximal expression ($P<0.05$), followed by intermediate levels in sporulated oocysts and merozoites ($P<0.05$ versus sporozoites), and minimal detection in unsporulated oocysts (Fig. 3B, C). These results demonstrate post-transcriptional regulation of *Et*RON2$_{L1-1}$ during parasite development.

Dynamic subcellular localization of *Et*RON2$_{L1-1}$ in *E. tenella*: Immunofluorescence assay revealed dynamic localization patterns of *Et*RON2$_{L1-1}$ across developmental stages. *Et*RON2$_{L1-1}$ protein was mainly localized in the cytoplasm in PBS-incubated sporozoites, but was translocated to the apical end following 2-hour incubation in complete medium (CM) or 2hrs post-invasion of DF-1 cells (Fig.4A-C). The fluorescence intensity was very weak in immature schizonts, while it increased significantly in mature schizonts (Fig.4D, E). In the second generation of merozoites, *Et*RON2$_{L1-1}$ protein is distributed throughout the cytoplasm and exhibits strong fluorescence intensity (Fig. 4F).

Anti-r*Et*RON2$_{L1-1}$ antibody mediates dose-dependent invasion inhibition: An invasion through an *in vitro* inhibition assay was carried out to address the role of *Et*RON2$_{L1-1}$ in *E. tenella* sporozoite invasion of DF-1 cells (Fig. 5). In comparison to normal rabbit IgG controls, anti-r*Et*RON2$_{L1-1}$ polyclonal antibody exhibited a dose-dependent inhibitory effect, with invasion rates significantly decreasing as antibody concentration increased ($P<0.05$). Specifically, treatment with 50μg/mL anti-r*Et*RON2$_{L1-1}$ resulted in a 13% inhibition rate, while 400μg/mL led to a 42% reduction in sporozoite invasion, demonstrating that *Et*RON2$_{L1-1}$ plays a critical role in host cell penetration.

***In vitro* characterization of constructed eukaryotic expression plasmids:** The target fragments of *Et*RON2$_{L1-1}$ and *Et*RON2$_{L2}$ were successfully amplified and cloned into eukaryotic expression vectors using a one-step cloning

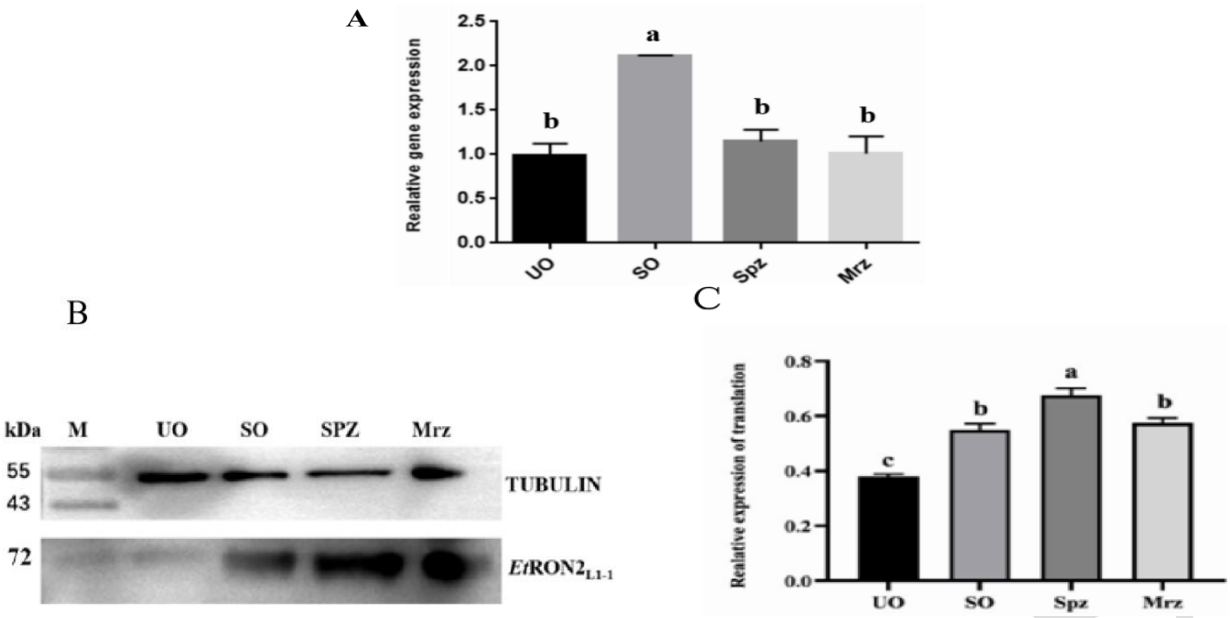

Fig.3: qPCR and western blot analysis of *Et*RON2$_{L1-1}$ expression during different *Eimeria tenella* developmental stages. UO: unsporulated oocysts; SO: sporulated oocysts; Spz: sporozoites; Mrz: second-generation merozoites. A. Levels of *Et*RON2$_{L1-1}$. B and C. Levels of *Et*RON2$_{L1-1}$.

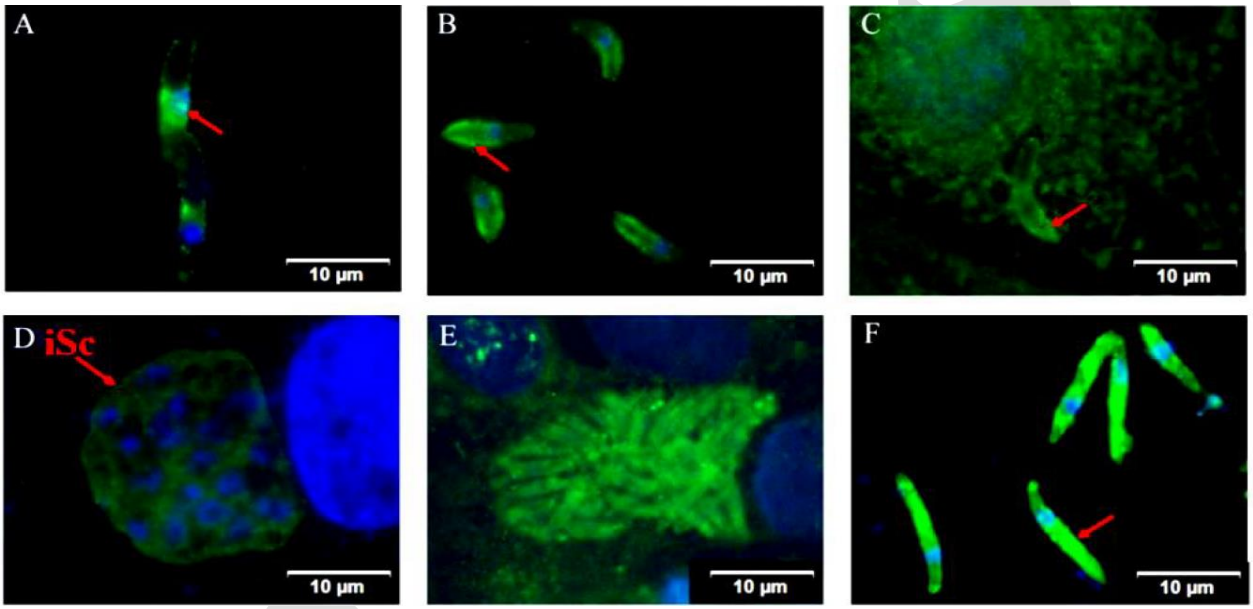

Fig.4: Indirect immunofluorescence localization of *Et*RON2$_{L1-1}$ at different developmental stages of *Eimeria tenella*. A: Sporozoites (Spz) in PBS; B: Spz in CM; C: Spz invade cells for 2h; D: Immature schizonts (iSc) at 60h, E: Mature schizonts at 72h; F: Second-generation merozoites in PBS.

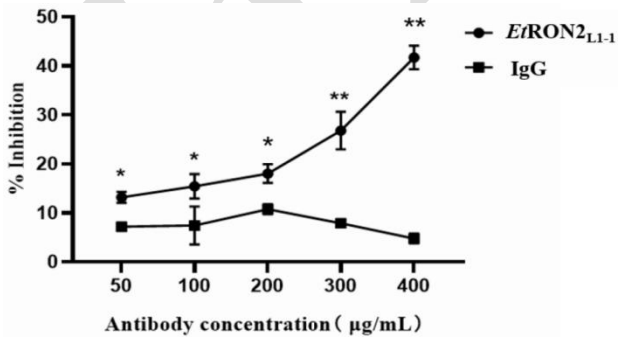

Fig. 5: Inhibition of sporozoite invasion *in vitro* by antibodies against r*Et*RON2$_{L1-1}$. *Et*RON2$_{L1-1}$ refers to rabbit antiserum generated against the recombinant *Et*RON2$_{L1-1}$ protein, while IgG represents serum from naive rabbits. Each experiment was conducted three times independently. Statistical significance is indicated as follows: a single asterisk (*) denotes a mean with P<0.05, and a double asterisk (**) indicates a mean with P<0.01.

method, generating recombinant plasmids pCAGGS-*Et*RON2$_{L1-1}$ and pCAGGS-*Et*RON2$_{L2}$ (Fig. 6A, B). Following 48h transfection of DF-1 cells, IFA confirmed efficient expression of both recombinant proteins. DF-1 cells whose transfection was done with either pCAGGS-*Et*RON2$_{L1-1}$ or pCAGGS-*Et*RON2$_{L1-1}$ exhibited strong, specific fluorescence signals (Fig. 7A-C), demonstrating successful *in vitro* expression of both *Et*RON2$_{L1-1}$ and *Et*RON2$_{L2}$ proteins. These results validate the functionality of both constructed plasmids for eukaryotic expression studies.

Protective effect of constructed plasmid vaccination to prevent *E. tenella*: To evaluate the vaccine potential of *Et*RON2$_{L1-1}$, this study employed *Et*RON2$_{L2}$, a previously characterized protective antigen (Liu *et al*., 2024), as a reference control for comparative assessment of anti-coccidial efficacy (Table 2). Challenge experiments revealed

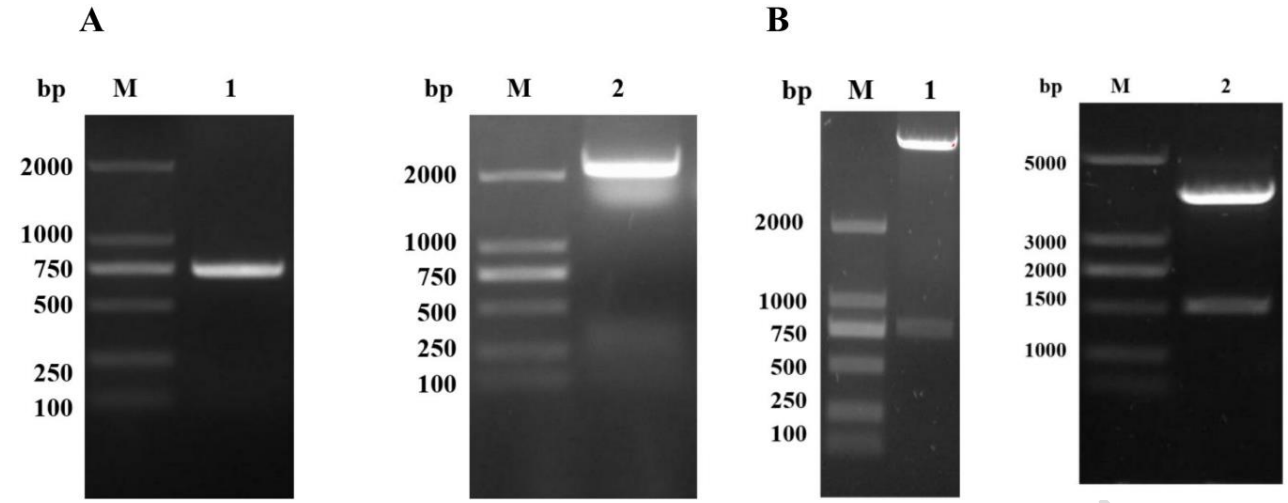

Fig. 6: Construction of eukaryotic expression plasmids pCAGGS-*Et*RON2$_{L1-1}$ and pCAGGS-*Et*RON2$_{L2}$. A: The results of PCR. M: DNA Marker (D$_{L2}$000); 1: *Et*RON2$_{L1-1}$; 2: *Et*RON2$_{L2}$. B: The results of double digestion. M: DNA Marker,1: pCAGGS-*Et*RON2$_{L1-1}$; 2: pCAGGS-*Et*RON2$_{L2}$.

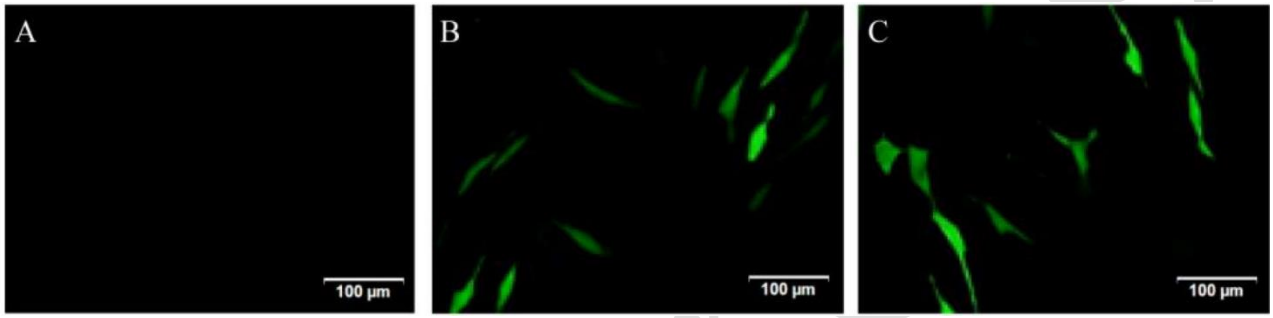

Fig. 7: Confirmation of the recombinant plasmids' expression in BHK cells. A: Negative control (pCAGGS transfected into BHK cells), B: pCAGGS-*Et*RON2$_{L1-1}$ transfected into BHK cells; C: pCAGGS-*Et*RON2$_{L2}$ transfected into BHK cells.

Table 2: Protective efficacy of constructed plasmid vaccination to prevent *E. tenella* in chickens

Groups	Weight gains during challenge (g)	Relative weigh gains (%)	Oocyst shedding (*10^7)	Oocyst reduction (%)	Lesion scoring
50μg *Et*RON2$_{L1-1}$	(187.90±37.79)^a	76.90	5.32^b	35.61	(1.71±0.34)^{ab}
50μg *Et*RON2$_{L2}$	(197.88±51.27)^{ab}	80.99	5.13^b	37.93	(1.48±0.54)^{bc}
50μg pCAGGS	(181.54±38.28)^a	74.30	7.96^a	3.63	(1.83±0.65)^a
100μg *Et*RON2$_{L1-1}$	(213.54±42.19)^b	87.39	6.44^b	22.02	(1.53±0.47)^{bc}
100μg *Et*RON2$_{L2}$	(215.01±46.44)^b	88.00	4.08^c	50.64	(1.36±0.21)^c
100μg pCAGGS	(190.53±47.57)^a	77.98	8.01^a	3.02	(1.75±0.41)^{ab}
Unvaccinated unchallenged	(244.34±25.19)^c	100.00	0	100.00%	0^d
Unvaccinated challenged	(178.59±44.76)^a	73.09	8.26^a	0	(1.85±0.72)^a

Note: In the same column, the same shoulder mark indicates no significant difference (P>0.05), and different shoulder marks indicate a significant difference (P<0.05). Values are presented as mean±standard deviation (n=14). Different superscript letters within the same column indicate significant differences (P<0.05) according to Duncan's multiple range test; groups sharing at least one identical letter (e.g., *ab*) are not significantly different from each other.

revealed that chickens immunized with 100μg doses of either pCAGGS-*Et*RON2$_{L1-1}$ or pCAGGS-*Et*RON2$_{L2}$ showed comparable weight gain (P>0.05), which was significantly higher than both the empty vector and non-immunized challenge groups (P<0.05). In contrast, the 50μg dose groups exhibited weight gain similar to control groups (P>0.05). Oocyst production was significantly reduced in all vaccinated groups compared to their corresponding empty vector controls (P<0.05), with the 100μg pCAGGS-*Et*RON2$_{L2}$ group demonstrating superior efficacy (P<0.05 versus pCAGGS-*Et*RON2$_{L1-1}$), while the 50μg groups showed comparable oocyst reduction (P>0.05). Intestinal lesion scores were significantly lower in both pCAGGS-*Et*RON2$_{L2}$ dose groups versus controls (P<0.05), whereas pCAGGS-*Et*RON2$_{L1-1}$ showed only a non-significant reduction. These results demonstrate *Et*RON2$_{L1-1}$'s partial but inferior protective efficacy compared to *Et*RON2$_{L2}$, identifying it as a candidate requiring further optimization for vaccine development.

DISCUSSION

Currently, drug resistance in chicken coccidiosis has become a widespread issue, and the application of live attenuated vaccines is limited due to problems such as virulence reversion and poor stability. Therefore, identifying novel vaccine candidates and developing effective vaccines is urgently needed. The RON2 protein family plays a crucial role in host cell invasion, virulence, and paraysitophorous vacuole modification in apicomplexan parasites, making it a promising vaccine candidate antigen (Lamarque *et al*., 2014). In this study, our sequence analysis demonstrated that while both *Et*RON2$_{L1-1}$ and *Et*RON2 contain three transmembrane domains, they

exhibit only 26.63% AA sequence homology. Notably, *Et*RON2$_{L1\text{-}1}$ lacks a signal peptide, whereas *Et*RON2 possesses an N-terminal Sec/SPI-type signal peptide (containing 1-28AA). These fundamental structural differences suggest distinct functional properties and potential mechanistic variations between these two related proteins in *E. tenella*.

Both transcriptional and translational analyses revealed stage-specific regulation of *Et*RON2$_{L1\text{-}1}$ through the whole life cycle of the parasite. At the protein level, *Et*RON2$_{L1\text{-}1}$ was nearly not measurable in unsporulated oocysts but showed significant expression in sporulated oocysts, sporozoites, and second-generation merozoites, with particularly abundant expression in sporozoites. Transcriptional profiling demonstrated the highest mRNA levels in sporulated oocysts, contrasting with lesser expression in merozoites, sporozoites, and unsporulated oocysts, a pattern distinct from *Et*RON2, which peaks in sporulated oocysts followed by merozoites (Li *et al*., 2024). The observed discordance between *Et*RON2$_{L1\text{-}1}$ transcriptional and translational profiles likely reflects post-transcriptional regulatory mechanisms, including mRNA processing, transcript stability, translational control, and post-translational modifications.

Immunofluorescence analysis revealed stage-specific subcellular localization of *Et*RON2$_{L1\text{-}1,}$ which was diffusely distributed in sporozoites, cytoplasm, and second-generation merozoites but became apically concentrated in intracellular sporozoites. Notably, *Et*RON2$_{L1\text{-}1}$ expression was markedly low in immature schizonts but significantly enhanced in mature schizonts, suggesting its potential involvement in both sporozoite invasion and schizont development. Consistent with this hypothesis, *in vitro* neutralization assays demonstrated that anti-*rEt*RON2$_{L1\text{-}1}$ antibodies effectively inhibited sporozoite invasion in a dose-dependent manner, showing significant inhibition at 50μg/mL ($P<0.05$) and reaching a 43% inhibition rate at 400μg/mL. In contrast, anti-r*Et*RON2 antibodies required higher concentrations (100–300μg/mL) to achieve significant invasion suppression ($P<0.05$) and exhibited no effect at 50μg/mL ($P>0.05$) (Li *et al*., 2024), indicating that *Et*RON2$_{L1\text{-}1}$ antibodies possess superior inhibitory efficacy compared to *Et*RON2 antibodies. These findings collectively highlight *Et*RON2$_{L1\text{-}1}$ as a critical virulence factor mediating host cell invasion and a potential target for intervention strategies.

Many RON2s from the Apicomplexa protozoan phylum have been identified as potential vaccine candidates, demonstrating efficacy in immune protection (Zhang *et al*., 2015; Cai *et al*., 2021; Patel *et al*., 2023). To assess the vaccine potential of *Et*RON2$_{L1\text{-}1}$, we constructed a chimeric subunit vaccine by cloning the *Et*RON2$_{L1\text{-}1}$ gene into the expression of the eukaryotic vector pCAGGS and determined its protective efficacy against *E. tenella* infection in chickens. *Et*RON2$_{L2}$, characterized protective antigen (Liu *et al*., 2024), was used as a reference control. The pCAGGS vector was selected for its strong transcriptional activity, featuring a cytomegalovirus enhancer coupled with a chicken β-actin promoter upstream of the multiple cloning site. This vector system has been successfully employed in numerous DNA vaccine studies, including those targeting infectious bursal disease virus (Li *et al*., 2013), avian influenza virus (Jiang *et al*., 2007), and duck tembusu virus (Xu *et al*., 2012). The immunization experiments demonstrated that chickens receiving 100μg of pCAGGS- *Et*RON2$_{L1\text{-}1}$ showed significantly improved weight gain and higher oocyst reduction rates compared to the empty vector group, while the 50μg group only exhibited significantly reduced oocyst output. However, both dosage groups showed no significant difference in cecal lesion scores versus controls, and their anti-coccidial effects were inferior to *Et*RON2$_{L2}$. These findings indicate that while *Et*RON2$_{L1\text{-}1}$ possesses dose-dependent anti-coccidial activity, its vaccine potential requires further optimization. However, a longer prime-boost interval is for DNA vaccines, which typically require longer to elicit adaptive immune responses, and can be considered in the coming studies. Another limitation of this study is that the immunogen was a C-terminally truncated fragment purified from inclusion bodies under denaturing conditions, and no refolding into a native-like conformation was performed. Antibodies raised against denatured fragments may primarily target linear epitopes; nonetheless, the ability of these antisera to detect *Et*RON2$_{L1\text{-}1}$ in parasite lysates (Western blot), to produce specific apical staining in IFA, and to inhibit sporozoite invasion functionally suggests they bind epitopes present on the native protein.

Conclusions: In conclusion, this study characterized *Et*RON2$_{L1\text{-}1}$ as a functionally distinct RON2 paralog in *E. tenella*, with unique structural features and critical roles in host cell invasion. While vaccination with *Et*RON2$_{L1\text{-}1}$ showed partial protective effects, its efficacy was inferior to *Et*RON2$_{L2}$. These findings highlight its potential as a vaccine candidate but emphasize the need for further optimization to improve its protective capacity against coccidiosis.

Funding: This work was supported by the Base and Talent Program of Science and Technology Plan in Tibet Autonomous Region (XZ202401JD0012).

Acknowledgements: We thank International Science Editing for editing this manuscript (http://www.internationalscienceediting.com).

Authors' contributions: WT, ML, XZ, BS, WQ, HD, and KL performed conceptualization and methodology. WT, ML, XZ, and BS performed software analysis validation, formal analysis, investigation, and data curation. WT performed writing—original draft preparation, Writing—review and editing, WT did visualization. WTL performed supervision, project administration, and funding acquisition. All authors have read and agreed to the published version of the manuscript.

Declaration of Competing Interest: The authors declare that they have no known competing financial interests or personal relationships that could have appeared to influence the work reported in this paper.

REFERENCES

Blackman MJ and Bannister LH, 2001. Apical organelles of Apicomplexa: biology and isolation by subcellular fractionation. Mol Biochem Parasitol 117(1):11-25.

Cai YC, Yang CL, Hu W, *et al.,* 2021. Molecular characterization and immunological evaluation of truncated *Babesia microti* Rhoptry Neck Protein 2 as a vaccine candidate. Front Immunol 12:616343.

Dong H, Yang S, Zhao Q, *et al.,* 2016. Molecular characterization and protective efficacy of silent information regulator 2A from *Eimeria tenella*. Parasit Vectors 9(1):602.

Dubois DJ and Soldati-Favre D, 2019. Biogenesis and secretion of micronemes in *Toxoplasma gondii*. Cell Microbiol 21(5):e13018.

Geysen J, Ausma J and Bossche HV, 1991. Simultaneous purification of merozoites and schizonts of *Eimeria tenella* (Apicomplexa) by percoll flotation and assessment of cell viability with a double fluorescent dye assay. J Parasitol 77(6):989–993.

Han H, Xue P, Dong H, *et al.,* 2016. Screening and characterization of apical membrane antigen 1 interacting proteins in *Eimeria tenella*. Exp Parasitol 170:116-124.

Ishino T, Murata E, Tokunaga N, *et al.,* 2019. Rhoptry neck protein 2 expressed in *Plasmodium* sporozoites plays a crucial role during invasion of mosquito salivary glands. Cell Microbiol 21(1):e12964.

Jiang LL, Lin J, Han HY, *et al.,* 2012. Identification and characterization of *Eimeria tenella* apical mem brane antigen-1 (AMA1). Plos One 7(7):e41115.

Jiang Y, Yu K, Zhang H, *et al.,* 2007. Enhanced protective efficacy of H5 subtype avian influenza DNA vaccine with codon optimized HA gene in a pCAGGS plasmid vector. Antiviral Res 75(3):234-41.

Johnson J and Reid WM, 1970. Anticoccidial drugs: lesion scoring techniques in battery and floor-pen experiments with chickens. Exp Parasitol 28(1):30-6.

Lal K, Bromley E, Oakes R, *et al.,* 2009. Proteomic comparison of four *Eimeria tenella* life-cycle stages: unsporulated oocyst, sporulated oocyst, sporozoite and second-generation merozoite. Proteomics 9(19):4566-76.

Lamarque MH, Roques M, Kong-Hap M, *et al.,* 2014. Plasticity and redundancy among AMA-RON pairs ensure host cell entry of *Toxoplasma* parasites. Nat Commun 5:4098.

Lee SK, Low LM, Andersen JF, *et al.,* 2023. The direct binding of *Plasmodium vivax* AMA1 to erythrocytes defines a RON2-independent invasion pathway. Proc Natl Acad Sci USA 120(1):e2215003120.

Li K, Gao L, Gao H, *et al.,* 2013. Codon optimization and woodchuck hepatitis virus posttranscriptional regulatory element enhance the immune responses of DNA vaccines against infectious bursal disease virus in chickens. Virus Res 175(2):120-7.

Li K, Gao L, Gao H, *et al.,* 2013. Protection of chickens against reticuloendotheliosis virus infection by DNA vaccination. Vet Microbiol 166(1-2):59-67.

Li Y, Zhang T, Liu X, *et al.,* 2024. *Eimeria tenella* rhoptry neck protein 2 plays a key role in the process of invading the host intestinal epithelium. Vet Parasitol 332:110322.

Lillehoj HS and Trout JM, 1993. Coccidia: a review of recent advances on immunity and vaccine development. Avian Pathol 22(1):3-31.

Liu MY, Zhu SH, Zhao QP, *et al.,* 2024. Preliminary characterization and functional analysis of the rhoptry neck protein *Et*RON2$_{L2}$ in *Eimeria tenella*. Chin. J Anim Infect Dis 32(4):1-10.

Oakes RD, Kurian D, Bromley E, *et al.,* 2013. The rhoptry proteome of *Eimeria tenella* sporozoites. Int J Parasitol 43(2):181-8.

Parker ML and Boulanger MJ, 2015. An extended surface loop on *Toxoplasma gondii* Apical Membrane Antigen 1 (AMA1) governs ligand binding selectivity. PLoS One 10(5):e0126206.

Parker ML, Penar*Et*e-Vargas DM, Hamilton PT, *et al.,* 2016. Dissecting the interface between apicomplexan parasite and host cell: Insights from a divergent AMA-RON2 pair. Proc Natl Acad Sci USA 113(2):398-403.

Patel PN, Dickey TH, Diouf A, *et al.,* 2023. Structure-based design of a strain transcending AMA1-RON2L malaria vaccine. Nat Commun 14:5345.

Robert-Gangneux F and Dardé ML, 2012. Epidemiology of and diagnostic strategies for toxoplasmosis. Clin Microbiol Rev 264-96. doi: 10.1128/CMR.05013-11. Erratum in: Clin Microbiol Rev 2012, 25(3):583.

Song X, Zhao X, Xu L, *et al.,* 2017. Immune protection duration and efficacy stability of DNA vaccine encoding *Eimeria tenella* TA4 and chicken IL-2 against coccidiosis. Res Vet Sci 111:31-35.

Sun H, Wang L, Wang T, *et al.,* 2014. Display of *Eimeria tenella Et*Mic2 protein on the surface of *Saccharomyces cerevisiae* as a potential oral vaccine against chicken coccidiosis. Vaccine 32:1869–1876.

Walker RA, Sharman PA, Miller CM, *et al.,* 2015. RNA seq analysis of the *Eimeria tenella* gametocyte transcriptome reveals clues about the molecular basis for sexual reproduction and oocyst biogenesis. BMC Genom 16:94.

Wang HX, Zhao QP, Zhu SH, *et al.,* 2021. Molecular characterization and functional analysis of *Eimeria tenella* citrate synthase. Parasitol Res 120:1025-1035.

Wang Q, Zhao Q, Zhu S, *et al.,* 2020. Further investigation of the characteristics and biological function of *Eimeria tenella* apical membrane antigen 1. Parasite 27:70.

Xu DW, Li GX, Li XS, *et al.,* 2012. Construction and immunogenicity of DNA vaccine encoding E gene of duck Tembusu virus. Chin J Prev Vet Med 34:30-38 (in Chinese).

Yan M, Huang B, Zhao QP, *et al.,* 2019. Interaction between domain 1 of apical membrane antigen 1 and rhoptry neck protein 2 in *Eimeria tenella* revealed by bimolecular fluorescence complementation assay. Chin J Anim Infect Dis 27(04):32-38.

Zhang T, Qu H, Zheng W, *et al.,* 2024. Oral vaccination with a recombinant *Lactobacillus plantarum* expressing the *Eimeria tenella* rhoptry neck 2 protein elicits protective immunity in broiler chickens infected with *Eimeria tenella*. Parasit Vectors 17:277

Zhang TE, Yin LT, Li RH, *et al.,* 2015. Protective immunity induced by peptides of AMA1, RON2 and RON4 containing T-and B-cell epitopes via an intranasal route against toxoplasmosis in mice. Parasit Vectors 8:15.

Zhou BH, Wang HW, Wang XY, *et al.,* 2010. *Eimeria tenella*: effects of diclazuril treatment on microneme genes expression in second-generation merozoites and pathological changes of caeca in parasitized chickens. Exp Parasitol 125:264-270.